The Astrophysical Journal, 714:1249–1255, 2010 May 10 doi:10.1088/0004-637X/714/2/1249

PHOTODISSOCIATION OF THE DIACETYLENE DIMER AND IMPLICATIONS FOR HYDROCARBON GROWTH IN TITAN'S ATMOSPHERE

Cunshun Huang[1], Fangtong Zhang[2], Ralf I. Kaiser[2], Vadim V. Kislov[3], Alexander M. Mebel[3], Ruchira Silva[1], Wilson K. Gichuhi[1], and Arthur G. Suits[1]
[1] Department of Chemistry, Wayne State University, Detroit, MI 48202, USA
[2] Department of Chemistry, University of Hawai'i at Manoa, Honolulu, HI 96822, USA
[3] Department of Chemistry and Biochemistry, Florida International University, Miami, FL 33199, USA
Received 2009 November 6; accepted 2010 January 12; published 2010 April 19

ABSTRACT

The surface of Titan is obscured by multiple aerosol layers whose composition and formation mechanism have remained poorly understood. These organic haze layers are believed to arise from photolysis and electron impact triggered chemistry in the dense nitrogen (N_2) and methane (CH_4) atmosphere involving highly unsaturated hydrocarbon molecules such as acetylene (HCCH), diacetylene (HCCCCH), and triacetylene (HCCCCCCH). Here we show via laboratory studies combined with electronic structure calculations that the photodissociation of the diacetylene dimer ($(HCCCCH)_2$) readily initiates atomic hydrogen loss and atomic hydrogen transfer reactions forming two prototypes of resonantly stabilized free radicals, C_4H_3 and C_8H_3, respectively. These structures represent hydrogenated polyynes which can neither be synthesized via traditional photodissociation pathways of the monomer nor via hydrogen addition to the polyynes. The photodissociation dynamics of mixed dimers involving acetylene, diacetylene, and even triacetylene present a novel, hitherto overlooked reaction class and show the potential to synthesize more complex, resonantly stabilized free radicals considered to be major building blocks to polycyclic aromatic hydrocarbons in Titan's low-temperature atmosphere.

Key words: astrochemistry – ISM: clouds – planets and satellites: general – planets and satellites: individual (Saturn, Titan)

Online-only material: color figures

1. INTRODUCTION

Titan's atmosphere exhibits an extensive aerosol haze believed to be composed of hydrocarbons and nitriles formed from its dense atmosphere (Coustenis et al. 1991; Yung et al. 1984; Lavvas et al. 2008; Wilson & Atreya 2004). Photochemistry and impact from magnetospheric electrons are believed to initiate a series of reactions involving the significant fraction of methane in the atmosphere. These pathways ultimately yield complex hydrocarbons and carbon–nitrogen based compounds through a series of reactions involving radicals and ions. These processes have remained poorly understood to date, although the haze is known to play a vital role in Titan's energy balance and atmospheric dynamics. Within the framework of the *Cassini–Huygens* mission, a wealth of new information is now becoming available that will help to shape our understanding of Titan's atmosphere and the mechanism of its hydrocarbon haze formation (Lebreton et al. 2005; Raulin & Owen 2002; Waite et al. 2007; Cravens et al. 2005; Vuitton et al. 2009; Coates et al. 2007).

Diacetylene (C_4H_2), the first of the series of polyynes, has long been recognized as a key species in Titan's atmosphere because it absorbs light at much longer wavelengths, where the solar flux is significant (Coustenis et al. 1991; Yung et al. 1984; Kunde et al. 1981), than acetylene, ethane, or other important trace constituents of the atmosphere. Diacetylene has long been thought to be central to the formation of higher polyynes and polycyclic aromatic hydrocarbons (PAHs) that partially comprise the haze layer in Titan's upper atmosphere (Yung et al. 1984; Vuitton et al. 2003, 2006). Reactions of metastable, electronically excited diacetylene were believed to play an important role in the formation of Titan's haze (Glicker & Okabe 1987; Silva et al. 2008; Arrington et al. 1998, 1999; Bandy et al. 1992, 1993; Frost et al. 1995). Recent work has suggested, however, that owing to its short lifetime and low dissociation rates, metastable diacetylene may not be significant in haze formation on Titan (Vuitton et al. 2003; Silva et al. 2008). In this report, we present an experimental and theoretical study of the photodissociation of the diacetylene dimer under collisionless conditions and show evidence that its photochemistry represents a novel, overlooked source of resonantly stabilized free radicals (RSFRs) in Titan's atmosphere. These are considered crucial building blocks in the synthesis of PAHs. Furthermore, the diacetylene dimer is just one example of a class of van der Waals complexes involving unsaturated hydrocarbons and nitriles that are likely to be sufficiently abundant to contribute to the hydrocarbon growth in Titan's atmosphere upon photochemical activation.

2. EXPERIMENTAL METHODS

The experiments were carried out on a crossed molecular beams apparatus described elsewhere (Gu et al. 2006). A pulsed molecular beam of diacetylene seeded in argon carrier gas was generated by supersonic expansion of a 5% mixture through a piezoelectric pulsed valve operating at 60 Hz and 80 μs pulses with 500 Torr backing pressure. A four-slot chopper wheel located between the skimmer and the cold shield selects a narrow segment of the seeded beam with a peak velocity of 567 ± 2 m s^{-1} and a speed ratio S of 8.3 ± 0.1. The expanded beam was skimmed twice before entering the main chamber, where it was crossed at 90° by a 193 nm photolysis laser. The time-of-flight (TOF) spectra of the photo fragments were recorded in the plane of both molecular and laser beams using a

rotatable quadrupole mass spectrometer with an electron-impact ionizer. Typically, the TOF spectra were recorded at lab angles in the range of 12°–35°. For all experiments, the delay time between the pulsed valve and the laser was set such that the diacetylene dimer signal was maximized relative to monomer and higher clusters. In trial experiments the laser was linearly polarized using a series of quartz plates at Brewster's angle. None of the photochemical signals were found to vary with laser polarization, so the experiments shown here were conducted with the laser unpolarized.

Diacetylene was synthesized using the method developed by Armitage et al. (1952). C_4H_2 was produced and collected in a cold trap at −70°C. After the synthesis, the sample was immediately transferred to a cylinder by slowly warming up the sample under vacuum. The cylinder was then filled to a total pressure of 3 bar with argon to produce 5% diacetylene mixture. The infrared absorption spectrum and mass spectrum showed high purity (>99.5%) using this synthesis.

The analysis of the TOF spectra at different laboratory angles was performed with a forward convolution program (Gu et al. 2006). A simulation of all measured TOF spectra was generated using an input center-of-mass P(E) distribution which was then convoluted over various instrument parameters such as beam velocity, laboratory angle, divergence of the beam, and so on. The P(E) distribution was iteratively adjusted until a satisfactory simulation was achieved.

The diacetylene dimer photodissociation to the product at $m/z = 51$ ($C_4H_3^+$) was also performed in DC slice imaging experiments. The apparatus and experimental procedure has been described in detail elsewhere (Huang et al. 2006; Townsend et al. 2003). Total translational energy distributions were derived from the sliced images by direct integration in velocity space, followed by conversion of the velocity distributions to translational energy. After carefully tuning the delay time between the diacetylene molecular beam and laser firing, the diacetylene dimer segments in the molecular beam were picked up and dissociated at 193 nm. Multiphoton ionization of the C_4H_3 product by the 193 nm laser allowed for detection. We were unable to detect $m/z = 99$ with this approach. Our detection of $m/z = 51$ may be through accidental 1+1 resonances, so the inability to detect $m/z = 99$ is not particularly surprising, as such resonances may not be available. Alternatively, ionization may not compete effectively with dissociation of the C_8H_3 neutral or other decay pathways in this case.

3. COMPUTATIONAL METHODS

Vertical excitation energies and transition dipole moments of diacetylene dimers were calculated using the equation-of-motion coupled clusters (EOM-CCSD) method (Stanton & Bartlett 1993; Rico & Head-Gordon 1993) with Dunning's augmented polarized triple-zeta correlation-consistent (aug-cc-pVTZ) basis set (Dunning 1989). For several lower energy excited states, we have also carried out internally contracted multireference configuration interaction (MRCI) calculations (Werner et al. 2003; Knowles & Werner 1988) with Davidson's corrections for quadruple excitations (MRCI+Q) and with active spaces including 8 electrons distributed on 8 orbitals (8, 8) and 16 electrons on 12 orbitals (16, 12). The (16, 12) active space involved all π electrons of the two diacetylene monomer units. The MRCI calculations were performed with the same aug-cc-pVTZ basis set. We considered two different structures of the diacetylene dimer, T-shaped and parallel-slipped; their optimized geometries were taken from the most accurate results by Hopkins et al. (2007) at the CCSD(T)/TZ2P(f, d)++ level of theory. Transition dipole moments were also computed at the complete-active-space self-consistent field CASSCF(16,12)/aug-cc-pVTZ level of theory (Werner & Knowles 1985; Knowles & Werner 1985). For comparison, similar EOM-CCSD, MRCI, and CASSCF calculations were performed for the isolated diacetylene molecule. In this case, we used (4, 4) and (8, 10) active spaces for MRCI and CASSCF. All ab initio calculations of excitation energies and transition dipole moments were carried out employing the MOLPRO 2006 program package (Werner 1996).

To unravel the reaction mechanism for the formation of the observed C_8H_3 + H and C_4H_3 + C_4H products in photodissociation of diacetylene dimer, we performed ab initio calculations of the ground state potential energy surface of C_8H_4 for various pathways leading from $(C_4H_2)_2$ to the products. Since the reaction paths lead from the species with a closed-shell singlet wave function (in the dimer) to the products having overall open-shell singlet wave functions, relevant intermediates and transition states may have a biradical character and therefore the use of multireference methods for the electronic structure calculations is required. Hence, we carried out geometry optimization and vibrational frequency calculations for various C_8H_4 species by employing the CASSCF approach with the active space consisting of 12 electrons distributed on 10 orbitals and the 6-311G** basis set, CASSCF(12,10)/6-311G**, and utilizing the Dalton 2 program package (Helgaker et al. 2005). Then, single-point relative energies were refined at the CASSCF-optimized geometries using the multireference second-order perturbation theory CASPT2 method (Werner 1996) implemented in MOLPRO 2006 (Werner et al. 2008) with the same active space and the cc-pVTZ basis set.

4. RESULTS

The diacetylene dimer was generated in a supersonic molecular beam, with photodissociation products probed via photofragment translational spectroscopy using two complementary approaches: universal mass spectrometric detection after electron-impact ionization (Gu et al. 2006) and non-resonant multiphoton ionization of the neutral products employing imaging detection (Huang et al. 2006; Townsend et al. 2003). The irradiation of the diacetylene beam at 193 nm gave rise to strong signals that were found to be associated with the photodissociation of the diacetylene dimer. Utilizing a universal mass spectrometric detector, the signal at a variety of mass-to-charge ratios (m/z) could be attributed to two reaction channels with unique contributions observed at $m/z = 51$ ($C_4H_3^+$) and $m/z = 99$ ($C_8H_3^+$). For completeness, we should mention that the dimer dissociation channel to form two diacetylene monomers ($m/z = 50$) was also observed. However, it is not discussed here in detail since the main interest of this project is to investigate the formation of RSFRs from the diacetylene dimers. Formally, channels at $m/z = 51$ ($C_4H_3^+$) and $m/z = 99$ ($C_8H_3^+$) correspond to the hydrogen loss and hydrogen transfer reactions (1) and (2), respectively, in the photodissociation process:

$$(C_4H_2)_2 + h\nu_{193\,\mathrm{nm}} \rightarrow C_8H_3 + H, \quad (1)$$

$$(C_4H_2)_2 + h\nu_{193\,\mathrm{nm}} \rightarrow C_4H_3 + C_4H. \quad (2)$$

When examined as a function of the delay time between the pulsed molecular beam valve and the laser, the profiles of the

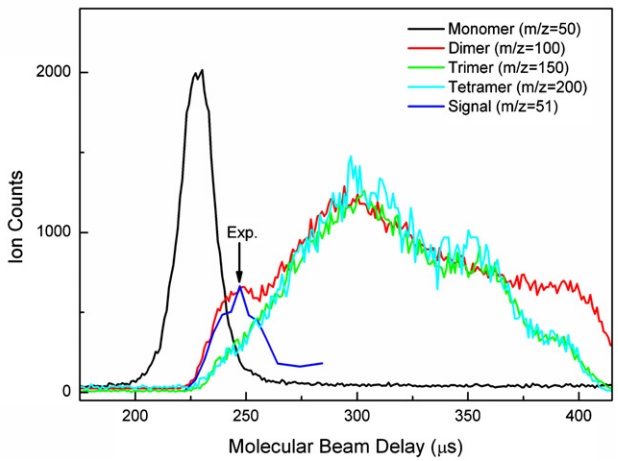

Figure 1. Signals on-axis in the molecular beam at indicated mass vs. delay between chopper and pulsed valves. The monomer contribution has been reduced by a factor of 80, while the other contributions have been normalized at long delay times.

(A color version of this figure is available in the online journal.)

product signals closely tracked the dimer appearance at $m/z = 100$, but not that of the monomer or higher clusters. These data are shown in Figure 1. The fact that the monomer, dimer, and cluster signals are shifted by the time of arrival at the detector is a manifestation of velocity slippage, which is readily observed here in part owing to the narrow velocity slice taken by the chopper wheel near the skimmer.

Representative TOF spectra at $m/z = 51$ and $m/z = 99$ are shown in Figure 2. This signal corresponds to products following hydrogen atom transfer from one diacetylene molecule to the other (reaction (2); $m/z = 51$) and from the hydrogen atom loss from the dimer (reaction (1); $m/z = 99$), respectively. The Newton diagrams are also shown to rationalize the maximum scattering range of the heavy reaction products of reactions (1) and (2). In these diagrams, the velocity of the diacetylene dimer beam is 567 m s^{-1}; the limiting circles depict the maximum recoil velocity calculated from the excitation energy at 193 nm and the reaction energies of the corresponding reaction channels (1) and (2) as discussed in detail below. The contribution at $m/z = 49$ includes both primary photochemistry corresponding

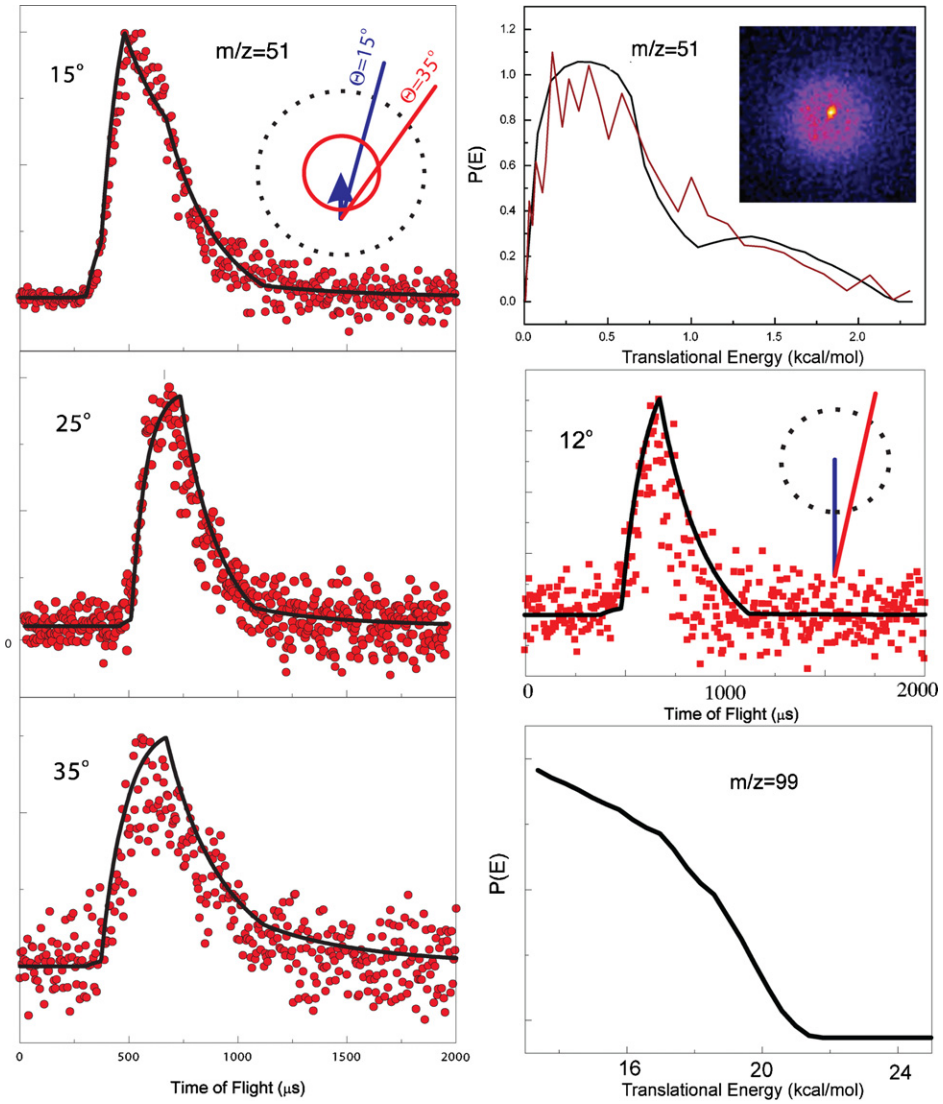

Figure 2. Representative TOF spectra recorded at mass-to-charge (m/z) of $m/z = 51$ ($C_4H_3^+$) and $m/z = 99$ ($C_8H_3^+$) fragments taken at indicated laboratory angles. The circles represent the data, while the solid lines depict the simulation based on the P(E)s, also shown in the figure. For the $m/z = 51$ case, ion imaging results are also shown, with the derived P(E) indicated by the lighter line. The Newton diagrams show the limiting center-of-mass velocities of the diacetylene dimer photodissociation product.

(A color version of this figure is available in the online journal.)

to the H transfer reaction, and fragmentation of $m/z = 50$ in the detector. As it is difficult to fit these contributions in a quantitative way, we do not show this result.

A forward convolution routine was used to fit the experimental data. Here, TOF spectra at $m/z = 99$ (C_8H_3) and $m/z = 51$ (C_4H_3) had to be fitted with a counter fragment of $m/z = 1$ (H) and $m/z = 49$ (C_4H) (reactions (1) and (2), respectively); the total mass of both reaction products of channels (1) and (2) of 100 amu also indicates that this signal originates from the diacetylene dimer. Likewise, the TOF spectra at $m/z = 99$ and 49 are distinct and do not overlap, demonstrating that at least two distinct channels are open in the photodissociation of the diacetylene dimer at 193 nm. This finding alone demonstrates that both channels lead to heavy hydrocarbon products of the gross formula C_8H_3 (reaction (1)) and C_4H_3 (reaction (2)). The corresponding center-of-mass translational energy (P(E)) distributions for both channels are also shown in Figure 2. The simulated TOF spectra are shown as the solid lines and the circles are the experimental data.

The product at $m/z = 51$ ((C_4H_3)) was also detected in a separate DC sliced ion imaging experiment. The image of the $C_4H_3^+$ ($m/z = 51$) photofragment was recorded and is shown as an inset in the center-of-mass translational distribution of $m/z = 51$ in Figure 2. In this case, the translational energy distributions were obtained by direct integration of the imaging data (Huang et al. 2006; Townsend et al. 2003). The translational energy distributions obtained for $m/z = 51$ in the two different experiments agree well, showing both a distribution maximum peaking away from zero and a high energy cutoff at about 2.3 kcal mol^{-1}. Therefore, the TOF spectra recorded at $m/z = 51$ and analysis support evidence of channel (2), i.e., the formation of two radical products with the gross formulae of C_4H_3 and C_4H.

The TOF spectrum recorded at $m/z = 99$ ($C_8H_3^+$) obtained with the universal detector shows that the atomic hydrogen loss channel, reaction (1), is also open in the photodissociation process. It is important to stress that we did not observe any signal at $m/z = 99$ at angles larger than 12°. At smaller laboratory angles, the signal was contaminated by background coming from the molecular beam itself. For $m/z = 99$, we thus only show the TOF spectrum at 12°. The total translational energy obtained from the forward convolution fitting is also shown in Figure 2; data are not reported below 13 kcal mol^{-1} because the results at 12° are not sensitive to slower recoiling fragments. In contrast to the translational energy distribution for the hydrogen atom transfer channel (reaction (2)), the translational energy distribution for the hydrogen atom loss channel (1) exhibits a broad distribution and extends to a higher kinetic energy release of about 25 kcal mol^{-1}.

Having established the existence of two pathways (1) and (2) to form two open-shell hydrocarbon radicals in the photodissociation of diacetylene dimers, via hydrogen transfer and hydrogen loss, of the generic formulae C_8H_3 and C_4H_3, we now examine the underlying photodissociation dynamics by considering the experimental results in light of high-level electronic structure calculations. This also helps to establish the extent to which the newly formed molecules belong to the class of RSFRs. This link is crucial to suggest possible structures of the isomers produced and to transfer these findings from the laboratory to the "real" atmosphere of Titan. Earlier high-level electronic structure calculations by Hopkins et al. suggest that the diacetylene dimer can either exist in a T-shaped or parallel-slipped configuration (Figure 3, Hopkins et al. 2007). The T-shaped dimer belongs to the C_{2v} symmetry point group whereas the parallel-slipped dimer has C_{2h} symmetry. The results of these calculations (Hopkins et al. 2007) give binding energies of T-shaped and parallel-slipped dimers of 1.63 ± 0.08 kcal mol^{-1} and 1.33 ± 0.12 kcal mol^{-1}, respectively, relative to two separated diacetylene monomers, making the T-shaped structure slightly more stable than the parallel-slipped one. According to the present ab initio calculations, electronic transitions in the dimers at 193 nm include excitation to the 1^1B_2, 2^1A_1, 3^1A_2, and 4^1A_2 states for the T-shaped form and 1^1B_u, 2^1A_u, 2^1A_g, and 2^1B_g for the parallel-slipped structure. Here the transitions to the 1^1B_2, 2^1A_1, 1^1B_u, and 2^1A_u states are electronically allowed, but those to 3^1A_2, 4^1A_2, 2^1A_g, and 2^1B_g are forbidden. Nevertheless, a strong vibronic coupling induced by the CCC and CCH bending modes is expected to contribute significantly to oscillator strengths of all these transitions and to make them vibronically allowed. The calculated vertical excitation energies for these states are about 5.5–5.6 eV; based on calculations of Franck–Condon factors, their absorption spectra represent vibrational progressions with the origin around 5.2–5.3 eV (the adiabatic excitation energy) and spaced by about 2300 cm^{-1}. Therefore, in addition to the electronic excitation, the absorption of a 193 nm photon produces vibrational excitation of the normal modes corresponding to the symmetric stretch of two triple carbon–carbon bonds coupled with the single carbon–carbon bond stretch with the frequency of about 2300 cm^{-1}.

The electronic structure calculations suggest further that photochemical activation by a 193 nm photon (148 kcal mol^{-1}) is likely followed by internal conversion (IC) to the (highly vibrationally excited) ground electronic state. Similar to diacetylene monomer (Silva et al. 2008), IC is expected to be fast. On the ground state potential energy surface, the individual diacetylene molecules within the dimers can be coupled via a carbon–carbon bond formation at the C4–C4 and C4–C3 positions leading to biradical intermediates **[i1]** and **[i2]**, respectively, with **[i1]** being thermodynamically more stable by 15 kcal mol^{-1} compared to **[i2].** It is important to stress that the energies of the transition states involved lie lower than the total available energy of the system. Formally, the parallel-slipped dimer correlates with the transition states leading to **[i1]** and **[i2]**. However, since the binding energies of the T-shaped and parallel-slipped dimers are low and the interaction between their monomer units is weak, isomerization between both structures is expected to be facile. The barrier for the parallel-slipped → T-shaped rearrangement cannot exceed 1.3 kcal mol^{-1} (the binding energy of the parallel-slipped structure), but it is likely to be much lower. Both **[i1]** and **[i2]** intermediates can isomerize via hydrogen shifts leading to **[i3]** and **[i4]**, respectively. Due to the change of the wave function character from the biradicals to the closed shell singlets, both structures are significantly more stable than **[i1]** and **[i2]**. Once again, the inherent barriers to hydrogen migration range well below the total available energy. The absolute barrier heights of 14–20 kcal mol^{-1} are reasonable when compared to similar closed shell, unsaturated hydrocarbon molecules (Mebel et al. 2006)). What is the fate of these reaction intermediates? Considering reactions (1) and (2), intermediate **[i3]** can either lose a hydrogen atom from the C3 position leading to a doublet C_8H_3 radical **p1** or undergo carbon–carbon bond rupture forming the *n*-C_4H_3 plus C_4H radicals. In intermediate **[i4]**, two decomposition pathways were identified as well: an atomic hydrogen loss leading to a C_8H_3 isomer **p2** and a carbon–carbon bond rupture forming the *i*-C_4H_3 radical plus the 1,3-butadienyl radical (C_4H). All processes involve only simple bond ruptures without

exit barriers. Note that among the C_8H_3 isomers, **p1** is thermodynamically more stable by about 12 kcal mol^{-1} compared to **p2**. The overall processes to form these isomers from the diacetylene dimers were found to be endoergic by 64 and 76 kcal mol^{-1}, for **p1** and **p2**, respectively. These energies are well below the total available energy of the system of 148 kcal mol^{-1}.

Considering the experimental data for the hydrogen loss channel (reaction (2)), the corresponding center-of-mass translational energy distribution (Figure 1) is broad, and around 80% of the available energy goes to internal excitation of the C_8H_3 products. This is consistent with the hydrogen loss translational energy distribution observed in the monomer (Silva et al. 2008), but those have only been reported at higher excitation energies, around 10.2 eV and above. This again highlights the important distinction between these monomer and dimer systems: the hydrogen atom elimination threshold for the dimer is 2.5–3.0 eV lower than for the diacetylene monomer. This is because the weak van der Waals bond in the dimer becomes a covalent bond in the product radical, thus gaining the bond energy and compensating partly for the large endoergicity of the bond fission. For the hydrogen atom transfer channel, which leads to two C4 radical species, the center-of-mass translational energy distribution is extremely low (<2 kcal mol^{-1}). This finding suggests that the effective transfer occurs with little direct interaction between the two monomers. This mechanism may be analogous to the dynamics of deuterium atom release reported in water dimer photodissociation (Kawasaki et al. 2004). A closer investigation of the overall reaction threshold exposes unique features of the dimer photodissociation. Here, the atomic hydrogen transfer mechanisms in the dimer, giving two C4 radicals, have a threshold of only 4.12 eV. No analogous channel exists in the monomer. A number of C_4H_3 product isomers are accessible (Mebel et al. 2006); the lowest energy pathways are shown in Figure 2 implying most likely the formation of *n*-C_4H_3 or *i*-C_4H_3. The very low observed translational energy release does not rule out any of these. It should be noted that such reactions of dimers are not unprecedented. Previous studies have demonstrated "sequential" and "concerted" dissociation of van der Waals complexes such as hydrogen iodide (HI) clusters (Chastaing et al. 2003), dimers of carbonyl sulfide (OCS; Van Veen et al. 1983) and carbon disulfide (CS_2; Tzeng et al. 1988), and the molecular oxygen (O_2) dimer (Brown & Vaida 1996). An overview of this literature is given in a recent study (Vidma et al. 2006).

An important question is the quantum yield for these processes relative to direct fragmentation of the dimer to yield monomer products. It is clear, simply based on the data in Figure 3, that a statistical prediction of the ground state branching would overwhelmingly favor the latter process, and the H transfer and H loss reactions from the dimer would be negligible. The fact that these channels are easily observed strongly suggests a role for reactions in dimer-excited states. Theoretical efforts are underway to investigate this.

5. DISCUSSION

Our combined experiments and calculations provide evidence that upon photolysis at 193 nm, the diacetylene dimer exhibits two unique reaction pathways leading to RSFRs, pathways that are absent in the photodissociation of the diacetylene monomer. These are the synthesis of the C_8H_3 isomers **p1** and/or **p2** via atomic hydrogen loss processes (reaction (1)) and the formation of *n*-/*i*-C_4H_3 isomers plus C_4H via carbon–carbon bond ruptures in the reaction intermediates (reaction (2)). Both pathways involved an initial formation of a carbon–carbon bond between the monomer units in the T-shaped and parallel-slipped dimer on the ground electronic state surface followed by an intermolecular hydrogen transfer. These processes represent direct evidence that the photoexcitation of weakly bound van der Waals structures such as the diacetylene dimer can lead to a hydrocarbon growth, in this case to the formation of RSFRs. This is in strong contrast to the diacetylene monomer, in which only photodestruction to the C_4H radical plus atomic hydrogen was observed.

Having verified hydrocarbon growth to form RSFRs in diacetylene dimer upon photoexcitation at 193 nm, we apply our findings now to the atmosphere of Titan. Previous models of Titan's atmosphere underline the crucial importance of RSFRs in the underlying reaction schemes leading to PAH formation (Yung et al. 1984; Lavvas et al. 2008; Wilson & Atreya 2004). Here, radicals such as C_4H_3, C_6H_3, and C_8H_3 were postulated as important transient species formed via addition of a hydrogen atom to a polyyne such as diacetylene (reaction (R1); Table 1). However, two major factors inhibit these reactions. First, classical activation barriers of the addition processes range from 2 to about 10 kcal mol^{-1}. Considering the temperature in Titan's stratosphere of about 120 K, the significant activation energy blocks the addition process at the outset. Second, the $[C_4H_3]^*$ reaction intermediate is internally excited; under the low-pressure regime in Titan's stratosphere of 10 mbar, a collisional stabilization of this complex via reaction (R2) by a bath molecule from the atmosphere, predominantly molecular nitrogen, is unlikely at these temperature and pressure conditions. A recent calculation by Klippenstein & Miller (2005) suggested very small rate constants of only about 1.8×10^{-26} cm^6 s^{-1} at 250 K to form C_4H_3 isomers. Considering the C_8H_3 radicals, the situation is even more complicated. Here, recent studies indicated that polyynes such as the tetraacetylene precursor itself (HCCCCC-CCCH; C_8H_2) can be synthesized via fast, barrierless reactions of diacetylene with ethynyl radicals (CCH) as formed in the photodissociation of acetylene at wavelengths less than 217 nm, followed by a consecutive reaction of a second ethynyl radical with triacetylene (HCCCCCCH; C_6H_2; reaction sequence (R4)–(R7)). The overall reaction (R8) formally converts two acetylene and one diacetylene molecule to tetraacetylene plus four hydrogen atoms. Alternatively, a reaction sequence could involve the reaction of photolytically generated 1,3-butadienyl radicals (reaction (R9)) with a diacetylene molecule (reaction (R10)). In analogy with reactions (R1) and (R2), the tetraacetylene molecule could only add a hydrogen atom over a significant barrier (reaction (R12)) followed by stabilization of the reaction intermediate (R13). Although the initial formation of tetraacetylene is fast, once again the hydrogen atom addition and stabilization of the intermediate, reactions (R12) and (R13), under Titan's atmospheric conditions are blocked. Therefore, the postulated reaction sequences (R1)–(R14) cannot lead to the formation of RSFRs in Titan's atmosphere due to the large activation energy, inefficient three-body processes, and the inherent small rate constants. A final possibility is the reaction of vibrationally excited ground state diacetylene monomers formed via nonradiative decay following photoexcitation. To our knowledge, this pathway has not been considered as a source of RSFR's in Titan's atmosphere to date. Its importance will depend on the reactivity of hot molecules, which we do not expect to be large, and on the vibrational cooling rates under the conditions in the stratosphere.

The diacetylene dimer is just one example of an overlooked reaction class involving van der Waals complexes consisting of

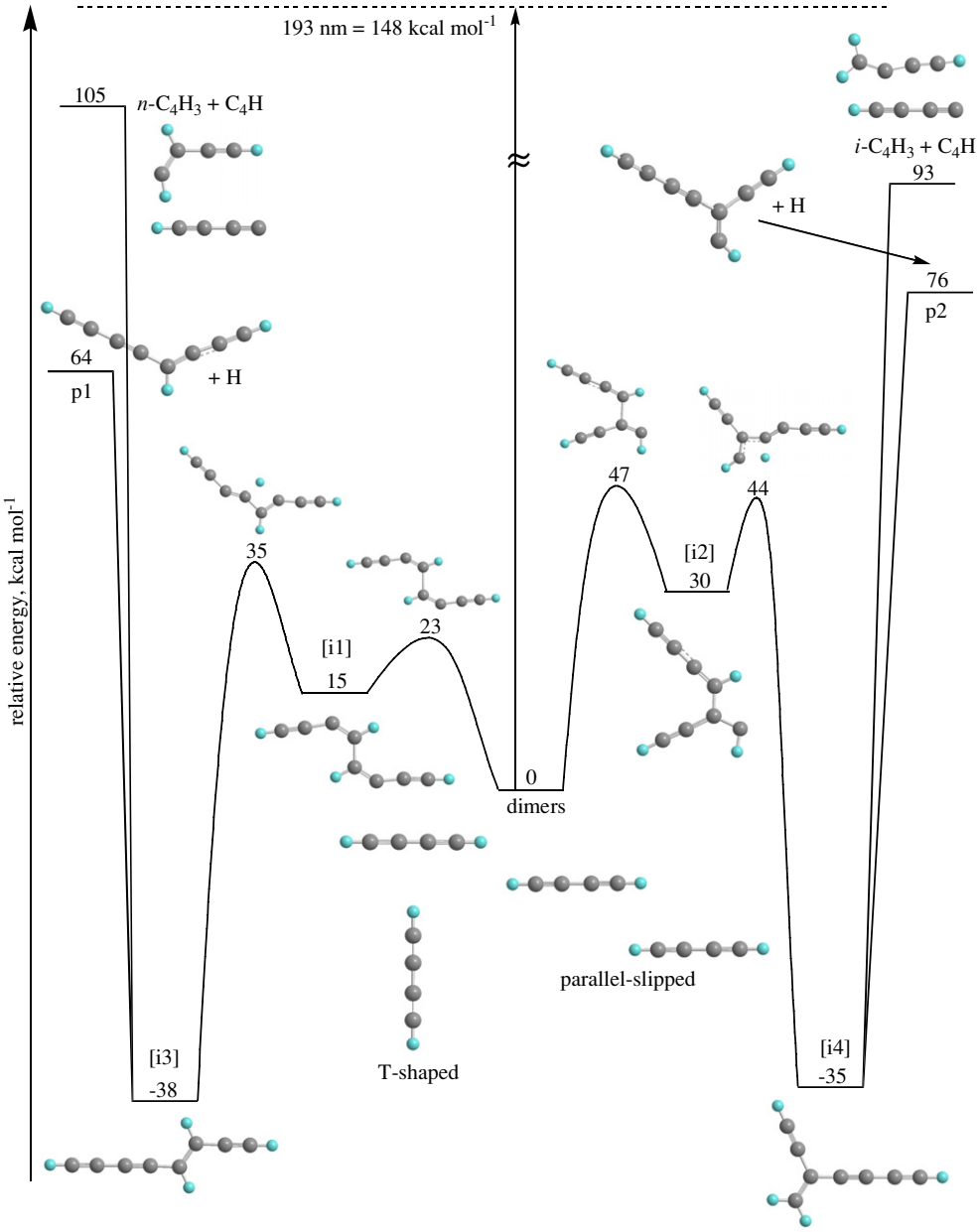

Figure 3. Stationary point on the potential energy surface involved in the photochemistry of the diacetylene dimer at 193 nm. The energies were calculated at the CASPT2(12,10)/cc-pVTZ//CASSCF(12,10)/6-311G** + ZPE(CASSCF(12,10)/6-311G**) level of theory.

(A color version of this figure is available in the online journal.)

Table 1
Compilation of Reaction Schemes in Titan's Atmosphere Postulated to be Involved in the Formation of Resonantly Stabilized Free Radicals via Hydrogen Atom Addition and Three-body Reaction Sequences

(R1)	$C_4H_2 + H \rightarrow [C_4H_3]^*$	(R4)	$C_2H_2 + h\nu \rightarrow C_2H + H$
(R1)	$[C_4H_3]^* + M \rightarrow C_4H_3 + M'$	(R5)	$C_2H + C_4H_2 \rightarrow C_6H_2 + H$
		(R6)	$C_2H_2 + h\nu \rightarrow C_2H + H$
		(R7)	$C_2H + C_6H_2 \rightarrow C_8H_2 + H$
(R3)	$C_4H_2 + H \rightarrow C_4H_3$	(R8)	$2\,C_2H_2 + C_4H_2 + 2\,h\nu \rightarrow C_8H_2 + 4\,H$
(R9)	$C_4H_2 + h\nu \rightarrow C_4H + H$	(R12)	$C_8H_2 + H \rightarrow [C_8H_3]^*$
(R10)		(R13)	$[C_8H_3]^* + M \rightarrow C_8H_3 + M'$
(R11)	$2\,C_4H_2 + h\nu \rightarrow C_8H_2 + 2\,H$	(R14)	$C_8H_2 + H \rightarrow C_8H_3$

polyynes and possibly cyanoacetylenes and aromatics that are likely to be sufficiently abundant to contribute to hydrocarbon growth in Titan's atmosphere upon photochemical activation. Analogous behavior is expected for acetylene, for example, and this is supported by calculations of the acetylene plus acetylene potential energy surface (Mebel et al. 2006). The acetylene dimer has an even stronger bond than the diacetylene dimer; therefore, the mixing ratios are expected to be much higher in

Titan's atmosphere for acetylene than diacetylene. Based on calculated equilibrium constants, we estimate mixing ratios of 6×10^{-14} for diacetylene dimer and 1×10^{-7} for the acetylene dimer in Titan's atmosphere at the 10 mbar level. The mixed acetylene–diacetylene dimer binding energy is comparable to that of diacetylene, but owing to the higher acetylene abundance on Titan, the mixed dimer mixing ratio is expected to roughly half that of the diacetylene monomer itself.

To summarize, the photodissociation of weakly bound van der Waals clusters of acetylenes and polyyacetylenes offer a mechanism to synthesize resonantly stabilized free radicals—building blocks toward the formation of PAHs—via a versatile one step pathway in Titan's low tempertature atmosphere. This presents a novel, neglected reaction class in chemical models simulating the growth of PAHs and of the organic haze layers on Titan and elsewhere in the outer solar system. Consequently, given the profound differences in photochemical behavior shown here, it is likely that the photodissociation of polyyne dimers such as reactions (1) and (2) leads to a more efficient formation of RSFRs than consecutive reactions involving hydrogen addition and three-body reaction sequences (R1)–(R14) in Titan's atmosphere. As the mixing ratios vary strongly with temperature and pressure, it will be important to include these complexes together with the wavelength-dependent quantum yield in future photochemical models to gauge the full extent of their role in the hydrocarbon growth on Titan.

The work was supported by the Collaborative Research in Chemistry Program of the US National Science Foundation (NSF-CRC CHE-0627854).

REFERENCES

Armitage, J. B., Jones, E. R. H., & Whiting, M. C. 1952, J. Chem. Soc., 2014
Arrington, C. A., Ramos, C., Robinson, A. D., & Zwier, T. S. 1998, J. Phys. Chem. A, 102, 3315
Arrington, C. A., Ramos, C., Robinson, A. D., & Zwier, T. S. 1999, J. Phys. Chem. A, 103, 1294
Bandy, R. E., Lakshminarayan, C., Frost, R. K., & Zwier, T. S. 1992, Science, 258, 1630
Bandy, R. E., Lakshminarayan, C., Frost, R. K., & Zwier, T. S. 1993, J. Chem. Phys., 98, 5362
Brown, L., & Vaida, V. 1996, J. Phys. Chem., 100, 7849
Chastaing, D., Underwood, J., & Wittig, C. 2003, J. Chem. Phys., 119, 928
Coates, A. J., et al. 2007, Geophys. Res. Lett., 34, L24S05
Coustenis, A., et al. 1991, Icarus, 89, 152
Cravens, T. E., et al. 2005, Geophys. Res. Lett., 32, L12108
Dunning, T. H. 1989, J. Chem. Phys., 90, 1007
Frost, R. K., Zavarin, G. S., & Zwier, T. S. 1995, J. Phys. Chem., 99, 9408
Glicker, S., & Okabe, H. 1987, J. Phys. Chem., 91, 437
Gu, X. B., Guo, Y., Mebel, A. M., & Kaiser, R. I. 2006, J. Phys. Chem. A, 110, 11265
Helgaker, T., et al. 2005, DALTON, a molecular electronic structure program, Release 2.0, http://www.kjemi.uio.no/software/dalton/dalton.html
Hopkins, B. W., ElSohly, A. M., & Tschumper, G. S. 2007, Phys. Chem. Chem. Phys., 9, 1550
Huang, C. S., Li, W., Kim, M. H., & Suits, A. G. 2006, J. Chem. Phys., 125, 121101
Kawasaki, M., et al. 2004, J. Phys. Chem. A, 108, 8119
Klippenstein, S. J., & Miller, J. A. 2005, J. Phys. Chem. A, 109, 4285
Knowles, P. J., & Werner, H.-J. 1988, Chem. Phys. Lett., 145, 514
Knowles, P. J., & Werner, H.-J. 1985, Chem. Phys. Lett., 115, 259
Kunde, V. G., et al. 1981, Nature, 292, 686
Lavvas, P. P., Coustenis, A., & Vardavas, I. M. 2008, Planet. Space Sci., 56, 27
Lebreton, J. P., et al. 2005, Nature, 438, 758
Mebel, A. M., KisIov, V. V., & Kaiser, R. I. 2006, J. Chem. Phys., 125, 133113
Raulin, F., & Owen, T. 2002, Space Sci. Rev., 104, 377
Rico, R. J., & Head-Gordon, M. 1993, Chem. Phys. Lett., 213, 224
Silva, R., et al. 2008, Proc. Natl Acad. Sci., 105, 12713
Stanton, J. F., & Bartlett, R. J. 1993, J. Chem. Phys., 98, 7029
Townsend, D., Minitti, M. P., & Suits, A. G. 2003, Rev. Sci. Instrum., 74, 2530
Tzeng, W. B., et al. 1988, J. Chem. Phys., 88, 1658
Van Veen, N. J. A., Brewer, P., Das, P., & Bersohn, R. 1983, J. Chem. Phys., 79, 4295
Vidma, K. V., Baklanov, A. V., Zhang, Y., & Parker, D. H. 2006, J. Chem. Phys., 125, 133303
Vuitton, V., et al. 2003, Planet. Space Sci., 51, 847
Vuitton, V., et al. 2006, Icarus, 185, 287
Vuitton, V., Yelle, R. V., & Lavvas, P. 2009, Phil. Trans. R. Soc. A, 367, 729
Waite, J. H., et al. 2007, Science, 316, 870
Werner, H.-J., & Knowles, P. J. 1985, J. Chem. Phys., 82, 5053
Werner, H.-J. 1996, Mol. Phys., 89, 645
Werner, H.-J., Manby, F. R., & Knowles, P. J. 2003, J. Chem. Phys., 118, 8149
Werner, H.-J., et al. 2008, MOLPRO, version 2008. 1, A package of ab initio programs, http://www.molpro.net
Wilson, E. H., & Atreya, S. K. 2004, J. Geophys. Res. Planets, 109, E06002
Yung, Y. L., Allen, M., & Pinto, J. P. 1984, ApJS, 55, 465